

Diffusion of water into permeation barrier layers

Bhadri Visweswaran, Prashant Mandlik, Siddharth Harikrishna Mohan, Jeff A. Silvernail, Ruiqing Ma, James C. Sturm, and Sigurd Wagner

Citation: *Journal of Vacuum Science & Technology A* **33**, 031513 (2015); doi: 10.1116/1.4918327

View online: <http://dx.doi.org/10.1116/1.4918327>

View Table of Contents: <http://scitation.aip.org/content/avs/journal/jvsta/33/3?ver=pdfcov>

Published by the AVS: Science & Technology of Materials, Interfaces, and Processing

Articles you may be interested in

[Modeling stress development and hydrogen diffusion in plasma enhanced chemical vapor deposition silicon nitride films submitted to thermal cycles](#)

J. Appl. Phys. **114**, 154113 (2013); 10.1063/1.4826208

[Fe diffusion in polycrystalline Cu \(In , Ga \) Se 2 layers for thin-film solar cells](#)

Appl. Phys. Lett. **96**, 244101 (2010); 10.1063/1.3449125

[Methods of producing plasma enhanced chemical vapor deposition silicon nitride thin films with high compressive and tensile stress](#)

J. Vac. Sci. Technol. A **26**, 517 (2008); 10.1116/1.2906259

[A single-layer permeation barrier for organic light-emitting displays](#)

Appl. Phys. Lett. **92**, 103309 (2008); 10.1063/1.2890432

[Lanthanum aluminate by atomic layer deposition and molecular beam epitaxy](#)

J. Vac. Sci. Technol. B **23**, 2480 (2005); 10.1116/1.2131077



Advance your technology or engineering career using the **AVS Career Center**, with **hundreds of exciting jobs** listed each month!

<http://careers.avs.org>



Diffusion of water into permeation barrier layers

Bhadri Visweswaran^{a)}

Department of Electrical Engineering and Princeton Institute for the Science and Technology of Materials, Princeton University, Princeton, New Jersey 08544

Prashant Mandlik, Siddharth Harikrishna Mohan, Jeff A. Silvernail, and Ruiqing Ma

Universal Display Corporation, Ewing, New Jersey 08618

James C. Sturm and Sigurd Wagner^{b)}

Department of Electrical Engineering and Princeton Institute for the Science and Technology of Materials, Princeton University, Princeton, New Jersey 08544

(Received 23 October 2014; accepted 6 April 2015; published 22 April 2015)

Organic light emitting diodes (OLEDs) are attractive candidates for flexible display and lighting panels due to their high contrast ratio. However, the materials in an OLED are oxidized by very small quantities of moisture. Therefore, flexible OLEDs require flexible, thin-film, encapsulation. The authors introduce a set of three techniques for measuring the solubility and diffusion coefficient of water in a permeation barrier layer that is a SiO₂-silicone hybrid made by plasma enhanced chemical vapor deposition. The techniques are secondary ion mass spectrometry, and measurements of electrical capacitance and of film stress. The measurements were carried out on samples exposed to water or steam at temperatures between 65 and 200 °C. From the resulting values of water solubility, diffusion coefficient, and their thermal activation energies, the authors calculate the time one monolayer of water will take to permeate through the bulk of the film. For a 3 μm thick film held at 38 °C and 90% relative humidity, the time is 13 years. © 2015 American Vacuum Society.

[<http://dx.doi.org/10.1116/1.4918327>]

I. FLEXIBLE BARRIERS FOR THE PROTECTION OF ORGANIC LIGHT-EMITTING DISPLAYS

Flexible organic light-emitting displays (OLEDs) require flexible permeation barrier films for their protection against atmospheric moisture and oxygen. Extremely small quantities of water can corrode the low-work function cathode, deactivate the emissive organic molecules, and oxidize the metal/organic interface in the OLED.¹ Yet OLED displays are expected to have operating lifetimes on the order of ten years. In today's rigid displays, the OLED is encapsulated together with a desiccant between two glass plates that are edge-sealed with a polymeric sealant.² While glass plates are excellent permeation barriers, they are rigid. Flexible glass sheets, which are thinner than 100 μm, have not yet entered display use. To make a display flexible, the bottom and top glass plates are replaced by a flexible substrate and a flexible encapsulation. The flexible substrate is made of polymers that allow water to permeate. Typically, the substrate is coated with a flexible barrier, the OLED is fabricated on it, and then the OLED in turn is coated with a flexible barrier; a foil of plastic is laminated with an adhesive over the top for mechanical protection and mechanical stress compensation.³ The flexible barrier film prevents the permeation of water into the OLED. Figure 1 is the schematic of such a structure.

The least-permeable and optically clear barrier materials are SiO₂, SiN_x, and Al₂O₃. However, when these materials are deposited as thin films in order to be flexible, they develop microcracks^{4,5} that render the films permeable. In addition, particulate contamination breaks the integrity of

the barrier films.^{6–8} In the conventional approach to solving these problems, alternating polymer layers and inorganic layers are deposited.^{9–11} The polymer layers mechanically decouple the adjacent inorganic layers. In particular, they decouple their microcracks such that microcracks in nearest-neighbor inorganic layers are not aligned with each other. The ensuing misalignment of microcracks makes the diffusion path for permeating atmospheric gas molecules very long. The polymer layers and the inorganic/polymer interfaces also can function as desiccants. Long diffusion paths combined with desiccation protect the OLED adequately.¹² Fabrication in this case is expensive due to the requirement of multiple deposition steps.

To reduce the time taken for film fabrication, we have been developing a single process barrier material that has very low permeability yet forms mechanically flexible and conformal films.¹³ The material is a SiO₂-silicone *hybrid* that is deposited by plasma-enhanced chemical vapor deposition (PECVD) from the source gases hexamethyldisiloxane (HMDSO) and oxygen. The properties of this hybrid material can be varied from SiO₂-like to silicone polymer-like, by

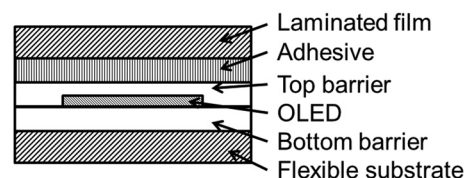


Fig. 1. Schematic cross-section of a flexible OLED panel made of a flexible polymer substrate, a bottom barrier layer, the OLED layers, a top barrier layer, an adhesive, and a top polymer foil.

^{a)}Electronic mail: bhadrinarayana.l.v@gmail.com

^{b)}Electronic mail: wagner@princeton.edu

varying the flow rates of HMDSO and oxygen and the radio frequency power that is fed into the glow discharge.¹⁴

We present a detailed study of the permeation of water into films made of one such SiO₂-silicone hybrid material that was deposited under one particular set of plasma conditions. Our study had three goals. The main goal was to predict the operating life of an encapsulated flexible OLED, when its lifetime is limited by exposure to water. The second goal was to explore and then introduce simple techniques for the evaluation of the permeability of water in a barrier layer. Our third goal was to learn as much as possible about the mechanism of water permeation, to put the lifetime model on a sound footing.

In the standard tests for evaluating OLED lifetime, encapsulated OLED devices are stored at elevated temperature and humidity in an environmental chamber. This is an accelerated test to identify and determine the rate of water induced degradation of the OLED. Typical pairs of temperature and relative humidity (*RH*) employed to accelerate aging are 85 °C and 85% *RH*, 65 °C and 90% *RH*, or 60 °C and 90% *RH*, respectively. The OLEDs under test are turned on periodically. When dark spots or bands appear in the luminescent area the OLED is considered to have failed. Typical targets for OLED lifetime in such accelerated tests are 500 or 1000 h. If an OLED shows no dark spot or band at the end of this period its encapsulation is considered adequate. This lifetime test, conducted directly on encapsulated OLEDs, has great advantages: it is highly sensitive, and it is realistic because it is conducted directly on the device that is to be protected. It has two drawbacks: One, the tests take three to six weeks, or even longer.¹³ The long delay between OLED encapsulation and test results seriously slows down the evaluation new or modified barrier materials and techniques.

The other drawback is that the OLED dark spot or band test does not distinguish clearly between the three pathways by which water can reach an encapsulated OLED. Water may penetrate (1) through the bulk of the barrier film, (2) through a microcrack or an embedded particle or along the interface between an embedded particle and the surrounding barrier material (causing circular dark spots), and (3) along the interface between the barrier film and its substrate (causing dark bands).¹⁵ Because the dark spot test does not inform about the inherent permeability of a barrier material, it cannot be used to efficiently guide material optimization. The same disadvantage applies to a similar and similarly sensitive test in which permeation is detected by the bleaching of an underlying reflective film of metallic calcium.^{16–18} In a group of widely employed tests of the permeability of free-standing barrier films, the flux of permeating gas is measured,¹⁹ but these tests are not sufficiently sensitive for the purpose, and also cannot discriminate between the three permeation mechanisms. With the exception of expensive ion beam techniques such as secondary ion mass spectrometry (SIMS), helium ion backscattering, and tritiated water permeation,^{20,21} none of the existing techniques can measure water permeation through the bulk of a barrier material at the level of sensitivity that OLEDs demand.

Therefore, we add two sensitive, simple, and rapid techniques for measuring the diffusion of water into a flexible barrier film, and to predict OLED lifetime from the diffusion results. The tests boil down to measuring the concentration profile of water that has diffused into the barrier material, and they can be carried out in less than a day. They consist of measuring the electrical capacitance of capacitors that use the barrier film, or of determining the mechanical film stress extracted from the radius of curvature of barrier film/silicon wafer couples. Both, capacitance and film stress, turn out to be highly sensitive and proportional to the amount of water dissolved in the barrier film. In both techniques, the samples need not necessarily reach steady-state permeation; hence, conclusive environmental tests can be carried out in very short times. The diffusion coefficient of water can be extracted from the results of capacitance and film stress measurements. To obtain the absolute value of water concentration, and of water concentration profiles, a measurement of the absolute water concentration is needed. One SIMS measurement will provide the water concentration.

We begin with a review of the parameters that characterize water permeation through barrier films, and how these parameters are used to specify barrier properties. Then we survey the literature on the mechanism of water diffusion into crystalline and fused silica, as these are the materials closest to the material of our barrier. We introduce the necessary diffusion equations. A description of the experimental techniques follows: measuring a water concentration profile by SIMS, and measuring step-by-step, between exposures to water, the electrical capacitance or the film stress. The PECVD process parameters employed to deposit the barrier film on substrates of glass, metallized glass, or silicon wafers are listed. Then we describe the procedures used to expose samples to liquid H₂O, D₂O, H₂¹⁸O, and superheated H₂O steam. The subsequent three sections describe the experimental results, discuss them, and use them to predict the one-monolayer permeation time τ_{ML} , which is our measure of OLED lifetime (1 monolayer = 10¹⁵ molecules/cm² of water).

II. PERMEATION BARRIER PROPERTIES AND REQUIREMENTS

The barrier quality of an encapsulation is captured by two properties: the steady-state permeability P and the water vapor transmission rate, $WVTR$. Both are evaluated at a specified temperature and a specified relative humidity. P is stated in units of g/cm s and $WVTR$ in g/m² day. In a barrier free of defects, P is the product of the diffusion coefficient D and the solubility S , of water at a given temperature and relative humidity. In contact with an inexhaustible source of water, the solubility S is also the concentration of dissolved water at the exposed barrier surface, n_0 . These and other symbols and units employed in this paper are listed in Table I. While the centimeter-gram-second (cgs) unit of g/cm³ is commonly employed for solubility when calculating P , we will use the solid-state electronics unit of molecules/cm³ because our targeted result is τ_{ML} , the permeation time

TABLE I. Symbols and units.

	Symbol	Units
Relative humidity	RH	%
Diffusion coefficient	D	cm^2/s
Complementary error function	erfc	—
Solubility and concentration in the surface	S or n_0	molecules/ cm^3
Normalized solubility	S_n	$\text{g}/\text{cm}^3 \text{ atm}$
Concentration	$n(x, t)$	molecules/ cm^3
Film thickness	h	nm
Time	t	seconds or hours or years
Total water dissolved in the film at time t	$N(t)$	molecules/ cm^2
Saturated total dissolved water at time $t = \infty$	$N(\infty)$	molecules/ cm^2
Permeability	P	$\text{g}/\text{cm s}$
Water vapor transmission rate	$WVTR$	$\text{g}/\text{m}^2 \text{ day}$
Oxygen transmission rate	OTR	$\text{cm}^3/\text{m}^2 \text{ day}$
Property such as capacitance or stress that is proportional to solubility of water	Π	Depends on specific property
Depth into the layer, from the surface	x	cm
Dry barrier dielectric constant	ϵ_0	—
Barrier dielectric constant	$\epsilon(x, t)$	—
Dielectric constant calibration factor	K_ϵ	$1/(\text{molecules}/\text{cm}^3)$
Capacitance at time t	$C(t)$	pF
Saturated capacitance	$C(\infty)$	pF
Area of the capacitor	A	cm^2
Surface stress	$\gamma(t)$	MPa cm
Film stress	$\sigma(t)$	MPa
Stress calibration factor	K_σ	MPa/(molecules/ cm^3)
1 monolayer permeation time	τ_{ML}	seconds or hours or years

for one monolayer of water molecules to reach the cathode. The normalized solubility S_n , expressed in $\text{g}/\text{cm}^3 \text{ atm}$, is the concentration of water in the barrier at the ambient water vapor pressure of $p_{H_2O} = 1 \text{ atm}$, at a specified temperature T . Below $T = 100^\circ\text{C}$, the normalized solubility S_n is calculated from measurements at the saturation vapor pressure of water $p_{H_2O} < 1 \text{ atm}$. The solubility S is assumed to be proportional to p_{H_2O} , following Henry's law. The permeation rate $WVTR$ is the diffusive flux of water through the barrier when its concentration gradient is uniform. $WVTR$ is calculated by dividing the permeability P at the given temperature and humidity by the thickness h of the barrier, $P/h = DS/h$. A widely quoted requirement for the allowable $WVTR$ of water into OLEDs is $10^{-6} \text{ g}/\text{m}^2 \text{ day}$ at room temperature. The equivalent requirement for the oxygen transmission rate (OTR) ranges from 10^{-5} to $10^{-3} \text{ cm}^3/\text{m}^2 \text{ day}$.^{3,22}

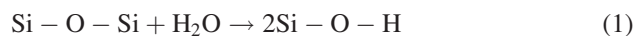
A barrier's life begins in as-deposited condition with zero extraneous water and eventually reaches steady-state when it transmits water at a constant rate, the $WVTR$. The time until steady-state is reached is called the "lag-time."¹² Currently, there are no established methods to exactly measure the failure quantity of water. One criterion employed for highly effective permeation barriers is that the lag-time be comparable or even longer than the required OLED lifetime.

However, defining the barrier lifetime as the lag-time derived from its $WVTR$ may lead to inaccurate lifetime estimates as is evident from Fig. 2. To set a precise value for the failure time, we use the time by which one monolayer of water has permeated through the barrier, τ_{ML} as the criterion, as shown in Fig. 2. τ_{ML} is the *lifetime* or *fail time*. Our target for the single-layer permeation barrier film is a τ_{ML} longer than 10 years. Permeation of one monolayer of water over 10 years corresponds to a $WVTR$ of $8.2 \times 10^{-8} \text{ g}/\text{m}^2 \text{ day}$ in steady state.

III. MECHANISM OF WATER DIFFUSION IN THE BARRIER MATERIAL

The hybrid barrier material of the present study has a chemical composition close to that of SiO_2 and, having been deposited from a glow discharge at low substrate temperature, is amorphous. Given that the HMDSO feedstock contains hydrogen, the plasma deposition process will introduce some hydrogen into the hybrid films. The films being amorphous, they are likely to contain strained bonds. Because of the hybrid's similarity to fused quartz we surmise that water diffuses through the barrier by a mechanism that is similar to that of water diffusion in fused quartz. The diffusion of water in crystalline and fused quartz has been studied extensively, and we adopt the analysis provided by Doremus²³ as it fits all of our results.

We summarize our conclusions on the diffusion mechanism at this point, to provide the rationale for analytical treatment of diffusion in Sec. IV. Experiments on the diffusion of H_2O into SiO_2 show that water enters by a diffusion-reaction mechanism. Two temperature regimes have been identified. At high temperatures, above 700°C , the reaction of water with the Si-O-Si network via



is fast. By enabling H_2O diffusion, the Si-O-H groups so formed dominate the rate of water diffusion. The network

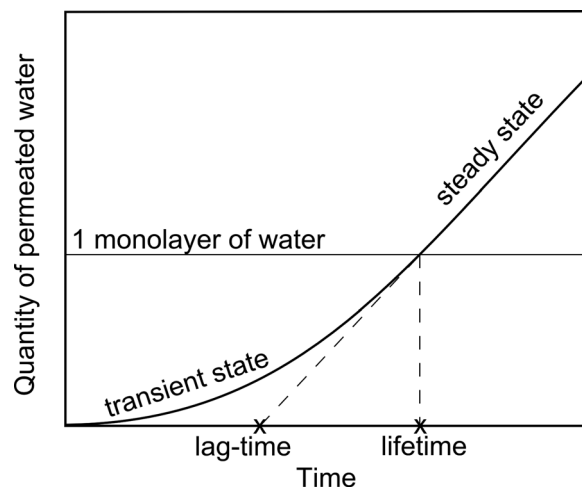


Fig. 2. Time taken for one monolayer of water to permeate and reach the OLED is defined as the "lifetime," τ_{ML} . The time taken for permeation rate to reach steady state is the "lag-time" (Ref. 12).

reacts with water first, thereby accelerating its diffusion. At low temperatures, the case we are studying, the fast process is diffusion of molecular H₂O, and local reaction with the Si-O-Si network follows. In other words, at low temperatures, the reaction is subsequent to diffusion. The interaction of water with the hybrid at low temperatures can be treated as simple diffusion of H₂O molecules instead of reaction-diffusion.

In general, water enters the hybrid material by a diffusion-reaction mechanism in which five processes participate.

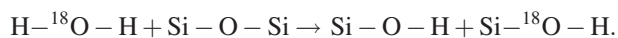
- (1) The surface concentration (activity) of water molecules $n(x=0) = n_0$ equilibrates with the partial pressure (fugacity) of water p_{H_2O} in the surrounding atmosphere.
- (2) Water molecules diffuse into the solid from the surface.
- (3) The hydrogen (when soaked in H₂O) or deuterium (when soaked in D₂O), but not oxygen, of the diffusing water molecules exchanges with the hydrogen of the Si-O-H groups of the SiO₂



- (4) The water molecules exchange oxygen in H₂O (or ¹⁸O in the case of H₂¹⁸O) by insertion into the Si-O-Si bonds, which then reconnect



- (5) H₂O (or H₂¹⁸O) molecules break Si-O-Si bonds permanently by insertion



Our experiments show evidence for processes 1–4, with process 1 being immediate and processes 3 and 4 occurring in local equilibrium with the diffusing water molecules. Processes 1–4 alone will result in a concentration independent diffusion mechanism. Process 4 is identified by tracking ¹⁸O isotopes. We shall also see that process 5 occurs only on a time scale so long that it does not affect OLED protection.

IV. ANALYSIS OF DIFFUSION AND APPLICATION TO FILM PROPERTIES THAT DEPEND ON WATER CONTENT

When a hybrid film is exposed to water, the film's electrical capacitance and mechanical stress increase over time. Both observations suggest that water diffuses into the film and changes its physical properties. The capacitance rises because the dielectric constant of H₂O is far higher than that of SiO₂. The film stress rises because H₂O causes the film to swell. The film however is constrained by its adhesion to the substrate, resulting in a stress build up. Fick's law of diffusion describes the diffusion of water into the film. Given its large surface area to thickness ratio, the film can be treated as a one-dimensional system with diffusion proceeding from $x=0$ at the film's surface to $x=h$ at the bottom surface of the film. The accumulation of water molecules in a given location, $n(x, t)$ and the water flux $J(x, t)$ at depth x in the barrier film are given by

$$\frac{dn(x, t)}{dt} = D \frac{d^2n(x, t)}{dx^2}, \quad (2)$$

and

$$J(x, t) = -D \frac{dn(x, t)}{dt}. \quad (3)$$

Here, $n(x, t)$ is the concentration of dissolved water molecules, t is the time, and D is the diffusion coefficient at depth x from the surface of the barrier ($x=0$). We will see that all diffusion data that we measured conform to solutions of Fick's laws, leading to a complementary error function (*erfc*) concentration profile of $n(x, t)$. The one exception is the ¹⁸O concentration profile after H₂¹⁸O soaks.

The barrier film surface quickly equilibrates with the ambient water. The surface concentration at $x=0$, n_0 , is equal to the solubility of water, S , at the test temperature and humidity. When n_0 of a semi-infinite sample ($\sqrt{Dt} \ll h$) is constant and H₂O diffuses without reacting with the Si-O-Si network, the concentration profile at time t is given by complementary error function

$$n(x, t) = n_0 \times \text{erfc}\left(\frac{x}{2\sqrt{Dt}}\right). \quad (4)$$

We now inspect two cases that are relevant to our study.

A. Barrier film deposited on an OLED

Two boundary conditions apply to a barrier film of thickness h on an OLED:

- (1) The top surface (at $x=0$) has a constant water concentration of n_0 that is set by the test temperature and relative humidity.
- (2) The OLED acts as a perfect sink for water. The concentration at the interface to the OLED (at $x=h$) is zero.

Solving Eq. (2) for these boundary conditions results in the total number of water molecules that has permeated into the OLED per unit surface area at time t , $Q(t)$, as given by Eq. (4.24) in Ref. 24

$$Q(t) = \frac{Dtn_0}{h} - \frac{hn_0}{6} - \frac{2hn_0}{\pi^2} \sum_{m=1}^{\infty} \frac{(-1)^m}{m^2} e^{-Dm^2\pi^2t/h^2}. \quad (5)$$

For long durations, Eq. (5) approximates as¹²

$$Q(t) = \frac{Dn_0}{h} \left(t - \frac{h^2}{6D} \right). \quad (6)$$

The WVTR and the lag time are hence expressed as

$$WVTR = \frac{Dn_0}{h}, \quad (7)$$

$$\text{Lag-time} = \frac{h^2}{6D}. \quad (8)$$

B. Barrier film deposited on an impermeable substrate

Water diffusion begins the same as in the OLED case, but the barrier film eventually saturates with water through its entire thickness. Then the film contains $N(\infty) = n_0 \times h$

molecules of water per unit surface area. At time t , the normalized number of water molecules absorbed by the permeation barrier, $N(t)$, is given by Eq. (4.18) in Ref. 24

$$\frac{N(t)}{N(\infty)} = 1 - \sum_{m=0}^{\infty} \frac{8}{(2m+1)^2 \pi^2} e^{-D(2m+1)^2 \pi^2 t / 4h^2}. \quad (9)$$

For short times, when $h \gg \sqrt{Dt}$, the expression above can be approximated as

$$N(t)^2 = 4 \left(\frac{N(\infty)}{h} \right)^2 \left(\frac{Dt}{\pi} \right). \quad (10)$$

Hence, D is given by

$$D = \left(\frac{h^2 \pi}{4N(\infty)^2} \right) \left(\frac{N(t)^2}{t} \right). \quad (11)$$

When $h \gg \sqrt{Dt}$, the diffusion coefficient D can be extracted by fitting the complementary error function of Eq. (4) to a measured concentration profile. Deuterated (D_2O) and tritiated water²⁵ have been used as markers to determine the diffusion coefficient of water and its solubility in silica glass in this manner. This is the quickest procedure for determining D when a SIMS profile is available.

Before the permeation barrier saturates with water, in other words when $\sqrt{Dt} < h$, the diffusion coefficient D can be extracted by measuring the total amount of dissolved water at time t , $N(t) = \int n(x, t) dx$ and the saturation quantity of dissolved water, $N(\infty)$. The diffusion coefficient is obtained from Eqs. (10) and (11). Equation (10) can also be employed to measure D in semi-infinite barriers if the surface concentration n_0 is known. In this case, Eq. (10) changes to

$$N(t)^2 = 4n_0^2 \left(\frac{Dt}{\pi} \right). \quad (12)$$

The weight of absorbed water is extremely small. For example, when a $1 \mu\text{m}$ thick barrier absorbs water at a concentration of 1% by weight, the barrier weight will increase by $2.66 \mu\text{g}/\text{cm}^2$. However, some chemical, electrical, and mechanical properties undergo substantial changes when water diffuses in. We identify a property Π that changes as a function of the total quantity of dissolved water $N(t)$. Π can be used to determine the diffusion coefficient. An inspection of Eq. (11) shows that the D can be extracted from measurements of any property that is proportional to N . By selecting the property that changes the most, the diffusion coefficient can be measured with high sensitivity. In our experiments, Π stands for a function of electrical capacitance C or mechanical film stress σ . When Π changes proportionally to $N(t)$ such that $(\Pi(t) - \Pi(0)) \propto N(t)$, Eq. (10) can be rewritten as

$$(\Pi(t) - \Pi(0))^2 = 4 \left(\frac{\Pi(\infty) - \Pi(0)}{h} \right)^2 \left(\frac{Dt}{\pi} \right). \quad (13)$$

Therefore, by measuring the *change* in chemical, electrical, or mechanical property Π at a fixed temperature and

humidity, the diffusion coefficient D can be evaluated. The thermal activation energy of the diffusion coefficient E_D can be calculated from diffusion coefficients D measured over a range of temperatures.

The thermal activation energies of S and $N(\infty)$ are stated for a fixed water vapor pressure p_0 . The small concentrations of water in the barrier of less than 1 mol. % justify two assumptions: the change in property Π varies linearly with the quantity of dissolved water molecules $N(t)$; and the proportionality constant relating them is temperature independent. Then, the thermal activation energy for the solubility of water E_S can be determined from $N(t = \infty, T)$. $N(t = \infty, T, p_{H_2O})$ is measured as a function of temperature and vapor pressure and then is normalized to a fixed water vapor pressure p_0 using $N(t = \infty, T) = N(t = \infty, T, p_{H_2O}) \times (p_0/p_{H_2O})$.

We assume that the concentrations of water established by exposure over the temperature range of our experiments (65–200 °C) do not change when the samples are brought to room temperature and then are evaluated in ambient atmosphere, or in vacuum as in a SIMS measurement.

V. BARRIER LAYER

The barrier layer evaluated in this paper is deposited at room temperature by PECVD from a gaseous mixture of HMDSO and oxygen.^{13–15} The deposition system has a radio frequency (13.56 MHz) powered triode configuration with an area of the powered center grid electrode of 182 cm^2 that is spaced 1 in. from the grounded substrate electrode, which faces downwards. A vapor mass flow controller feeds HMDSO vapors preheated to 33 °C. This HMDSO vapor is premixed with oxygen before it is fed into the deposition chamber. By varying gas flow rates, pressure, electric power fed into the discharge, and substrate temperature, the barrier material properties can be varied widely between essentially pure SiO_2 to those of plasma-polymerized HMDSO. The layers made for the current study were deposited with mass flow rates of 1.1 sccm of HMDSO vapor, 33 sccm of O_2 , at a chamber pressure of 110 mTorr and with the substrate holder at nominal room temperature. A detailed study of PECVD deposition rate, wet and dry etch rates, infrared absorption spectra, water droplet contact angle, surface roughness and phase shift in atomic force microscopy, coefficient of thermal expansion, critical tensile strain, elastic modulus, indentation hardness, optical absorption spectrum, refractive indices, relative dielectric constants, and electrical conduction has been published.¹⁴ Desired film properties are tuned to application requirements such as conformable coating of surface profiles and of incidental particles, desired radius of curvature during bending and rolling, film stress and film stress compensation. Films of essentially silicon dioxide yet with a small residual carbon content are highly impermeable yet flexible.

VI. EXPERIMENTS AND DATA EXTRACTION

All samples were exposed to water in the same way. At temperatures greater than 100 °C up to 200 °C, the samples were held in superheated steam at 1 atm pressure. At

temperatures from 65 to 100 °C, the samples were kept in water. The temperature determines the rate at which the water diffuses and in turn the rate of change in electrical capacitance and film stress. Temperature and humidity together determine the solubility of water, S or n_0 , in the barrier.

A. Secondary ion mass spectroscopy

The hybrid material contains a background concentration of native hydrogen introduced by PECVD from HMDSO. This background concentration is of the order of 10^{20} atoms/cm³, which is comparable to the surface concentrations of H added during the diffusion experiments. To distinguish between the native and in-diffused hydrogen, we exposed one SIMS sample to heavy water, D₂O, and evaluated the concentration profiles of both hydrogen and deuterium. The natural abundance of D in water of only 0.016 at. % is so low that it does not affect our results. The situation is different for ¹⁸O introduced by exposure to H₂¹⁸O, which we measured to identify O exchange with the Si-O-Si network. The concentration of O in SiO₂ is 67 at. %, and the natural abundance of ¹⁸O is 0.20 at. %. Therefore, the ¹⁸O concentration in SiO₂ is 0.13 at. %, which is comparable to the surface concentration reached with in-diffused H₂¹⁸O.

Two samples were evaluated by SIMS: One had been held in boiling heavy water (D₂O) and the other in boiling H₂¹⁸O. The samples were exposed briefly enough to ensure $\sqrt{Dt} \ll h$. Then, the concentration of water follows a complementary error function distribution with a diffusion coefficient D given by Eq. (4).

B. Electrical capacitance

The as-deposited permeation barrier material has a dielectric constant of $\epsilon_0 = 3.9$, the same as SiO₂.¹⁴ Because water molecules are highly polarizable, they can raise the dielectric constant of the barrier material considerably even when dissolved in small quantities. In capacitors made with the barrier as the dielectric (Fig. 3), the capacitance rises upon exposure to water. As in humidity sensors made with dielectric of organic polymers,²⁶ the capacitance rises linearly with rising partial pressure of water. In our case, the highest concentration that water reaches is small, of the order of 1 at. %. Because the uptake of water has a much bigger effect on the dielectric constant than on the layer thickness h , we assume that h is constant. The dielectric constant

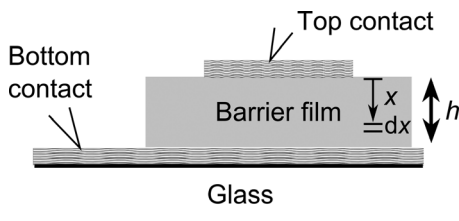


Fig. 3. Schematic cross section of capacitors with the barrier material as dielectric. The capacitance change upon exposure to water is monitored to extract the diffusion coefficient D . The top contact is made of a thin porous chromium film.

$\epsilon(x, t)$ of a homogeneous mixture of a host with dielectric constant ϵ_0 with a solute of concentration $n(x, t)$ is given by Landau and Lifshits²⁷

$$\epsilon(x, t) = \epsilon_0(1 + K_\epsilon \times n(x, t)). \quad (14)$$

Simple linear expressions of this form are also valid for inhomogeneous mixtures that contain small quantities of a second phase.²⁸

To understand how water in-diffusion affects the capacitance of the structure, let us analyze a capacitor of thickness h , given by Fig. 3. An infinitesimally thin slab of thickness dx at a depth of x at time t contains a small concentration $n(x, t)$ of molecularly dissolved water. The local dielectric constant is given by Eq. (14). For a capacitor of area A and thickness h , the capacitance at time t is then given by

$$\frac{1}{C(t)} = \int_0^h \frac{dx}{A\epsilon_0(1 + K_\epsilon n(x, t))}. \quad (15)$$

For a given temperature T and water vapor pressure p_{H_2O} , the surface concentration of water stays constant at $n_0 = n_0(T, p_{H_2O})$ throughout the experiment. The thickness of the capacitor, h , is assumed to be constant as it is minimally raised by swelling. The concentration of water in the dielectric $n(x, t)$ at depth x and time t is given by the complementary error function distribution of Eq. (4). We reformulate Eq. (15) with a Taylor expansion around $K_\epsilon n_0 = 0$ and drop the second and higher order terms to get

$$\frac{1}{C(t)} = \int_0^h \frac{dx}{A\epsilon_0} \left(1 - K_\epsilon n_0 \operatorname{erfc} \left(\frac{x}{2\sqrt{Dt}} \right) \right) dx. \quad (16)$$

Since the concentration profile is far from steady state, $\sqrt{Dt} \ll h$, the upper limit of the integral is extended to ∞ ; then the change in the inverse capacitance is linear in the square root of time

$$\left(\frac{1}{C(0)} - \frac{1}{C(t)} \right) = \left(\frac{K_\epsilon n_0}{hC(0)} \right) \times \frac{2\sqrt{Dt}}{\sqrt{\pi}}. \quad (17)$$

Rewriting Eq. (15) for time $t = \infty$ when the capacitor is saturated with water, $n(x, t) = n_0$, yields

$$K_\epsilon n_0 = \frac{C(\infty) - C(0)}{C(0)}. \quad (18)$$

This result enables eliminating the unknowns in Eq. (17)

$$\left(\frac{1}{C(0)} - \frac{1}{C(t)} \right)^2 = \left(\frac{C(\infty) - C(0)}{C(0)^2} \right)^2 \times \frac{4D}{h^2\pi} \times t. \quad (19)$$

Therefore, measuring the initial capacitance $C(0)$, the capacitance $C(t)$ at time t of water exposure, and the capacitance of a sample saturated with water $C(\infty)$ provides the data needed for evaluation of the diffusion coefficient D . Equation (19) is valid as long as the concentration of water

$n(x, t)$ is small and the diffusion coefficient is independent of concentration, $n(x, t)$. The constant K_c is calibrated against the solubility, n_0 , obtained through secondary ion mass spectrometry using Eq. (14).

C. Mechanical stress

As water permeates a barrier film, the barrier film swells. When the film is bonded to a substrate, the swelling is constrained. Therefore, the surface stress γ increases in the barrier film and adds to the built-in surface stress $\gamma(0)$ that results from the film deposition. The change in surface stress upon water exposure, $\gamma(t) - \gamma(0)$, is proportional to the quantity of dissolved water $N(t)$

$$\gamma(t) - \gamma(0) = K_\sigma \times N(t). \quad (20)$$

Hence, for a barrier of thickness h and surface concentration n_0 , upon saturation, the change in surface stress becomes

$$\begin{aligned} \gamma(\infty) - \gamma(0) &= K_\sigma \times N(\infty) \\ &= K_\sigma \times n_0 \times h. \end{aligned} \quad (21)$$

The stress, $\sigma(t) = \gamma(t)/h$, is the surface stress per unit thickness of the barrier. Hence, the change stress in the barrier film saturated with water is given by $\sigma(\infty) - \sigma(0) = K_\sigma \times n_0$.

The silicon wafer bends in response to the surface stress. The stress $\sigma(t)$ at time t is calculated from the bending radius of curvature, $R(t)$, of the silicon wafer containing the barrier film at time t , with respect to the bare silicon wafer using the Stoney²⁹ equation. $R(0)$ and $\sigma(0)$ are the bending radius of curvature and mechanical stress, respectively, of the as-deposited sample, at time $t=0$. E_w and h_w are the elastic constant and thickness, respectively, of the silicon wafer

$$\sigma(t) = \frac{E_w h_w^2}{6R(t) h}. \quad (22)$$

The change in stress is linear with the water uptake $N(t)$. Hence, $(\Pi(\infty) - \Pi(0))$ of Eq. (13) is replaced with the change in stress $(\sigma(\infty) - \sigma(0))$ to obtain

$$(\sigma(t) - \sigma(0))^2 = 4 \left(\frac{\sigma(\infty) - \sigma(0)}{h} \right)^2 \left(\frac{Dt}{\pi} \right). \quad (23)$$

By measuring the change in stress of the barrier and its saturation value, the diffusion coefficient of water can be found.

We use measurements of mechanical stress over a range of temperatures to evaluate the thermal activation energy of solubility (or surface concentration) and diffusion coefficient of water. The solubility is proportional to the saturated stress. The thermal activation energy of solubility is measured from dependence on temperature of the saturated stress $(\sigma(\infty) - \sigma(0))/p_{H_2O}$, normalized to 1 atmosphere water vapor pressure.

VII. EXPERIMENTAL PROCEDURES

The SIMS and electrical capacitance samples were held in boiling water, i.e., at 100 °C and 100% relative humidity.

For stress measurement, the samples were exposed to temperatures ranging from 65 to 200 °C, to obtain temperature dependences of solubility and the diffusion coefficient. For temperatures below 100 °C, the samples were immersed in water. For temperatures above 100 °C, the samples were placed on a temperature controlled hot plate. An inverted funnel was placed over the sample. A boiler generates steam which was fed into the stem of the funnel and on the way was super-heated to the same temperature as the hot plate. The vapor pressure remains at 1 atmosphere because the funnel rests loosely on the hot plate. For time series of stress measurements, the samples were taken off the hot plate and cooled down to the fixed room temperature of 22 °C before measurement.

A. SIMS measurement

To measure solubility and determine the diffusion coefficient by SIMS, 660 nm barrier films were deposited on 100 mm diameter, 500 μm thick, $\langle 100 \rangle$ oriented silicon substrates. One wafer was exposed to D_2O and another to H_2^{18}O . The deuterium and hydrogen concentrations were calibrated against ion implanted thermally grown silicon dioxide samples. The samples were held in a boiling deuterium oxide bath at 101 °C for 12 h, and in boiling H_2^{18}O for 4 h, respectively. The bath is fitted with a reflux condenser that traps any escaping deuterium oxide or H_2^{18}O steam. The sputter profile area for the SIMS experiments was 125 $\mu\text{m} \times 125 \mu\text{m}$.

The raw ^{18}O data from SIMS were obtained in the form of counts. Natural ^{18}O abundance is 0.2 at. %. Therefore, the expected natural ^{18}O concentration in SiO_2 is 9×10^{19} atoms/ cm^3 . The background ^{18}O concentration measured in counts was calibrated with the known natural ^{18}O atomic concentration in silicon dioxide.

B. Electrical capacitance

The capacitors were fabricated by sputter depositing a 100 nm chromium bottom contact on a glass substrate. A 200 nm blanket permeation barrier layer was deposited over this bottom electrode, following which a thin 15 nm top chromium contact was deposited through a shadow mask. The top chromium contact is porous and does not slow down the diffusion of water into the capacitor structure. It has an area of $0.79 \times 10^{-2} \text{ cm}^2$. Shadow masking instead of photolithography was used to prevent any exposure of the sample to solvents while at elevated temperatures during lithography, when diffusing-in solvents and water may alter the dielectric constant of the barrier prior to the actual diffusion experiment. The capacitors were held in boiling water. The capacitance was measured at 1 MHz with an Agilent 4275A LCR meter after taking the capacitor out of the boiling water and thoroughly blow drying it with nitrogen. The procedure is repeated at time intervals to obtain the time dependence of sample capacitance.

C. Mechanical stress

To measure the diffusion properties by monitoring mechanical stress, 1.5 μm thick permeation barrier layers were

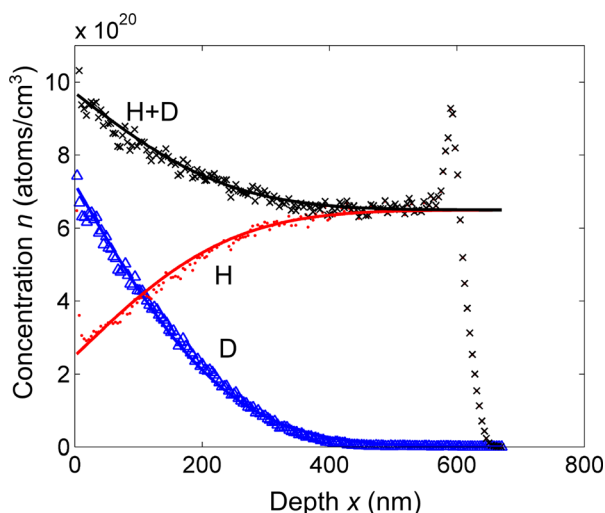


FIG. 4. (Color online) Hydrogen, deuterium, and hydrogen+deuterium SIMS profiles measured in a 660 nm thick barrier on a silicon wafer after exposure to 101 °C boiling D_2O for 12 h. All solid lines are complementary error function fits with a D value of $4.2 \times 10^{-15} \text{ cm}^2/\text{s}$. Table II gives the measured concentrations and diffusion coefficients.

deposited on $\langle 100 \rangle$ oriented, $525 \mu\text{m}$ thick silicon wafers. The bending radius of curvature of the wafer was obtained by profiling the silicon wafer before and after barrier film deposition, and after time intervals during water experiment using a KLA Tencor P-15 profilometer. The thickness h of the barrier on the silicon dioxide was measured using a Nanospec reflectometer. From the bending radius of curvature, the stress in the barrier film was calculated from Eq. (22). The as-deposited film is compressive. The initial stress of the wafer was calculated. The change in stress in the wafer upon water diffusion was calculated by subtracting the initial stress in the wafer from the total stress.

The accelerated test condition was varied from 65 to 200 °C while keeping the entire experimental setup at 1 atmosphere total pressure. For temperatures below 100 °C, the barrier on silicon wafer was immersed in a constant temperature water bath, which we consider the equivalent of exposing the barrier to 100% relative humidity.

To extract the diffusion coefficient, the saturated stress of the wafer, $\sigma(\infty)$, also needs to be measured. This experiment is quick at high temperatures as water diffuses in and saturates the entire barrier thickness of $1.5 \mu\text{m}$ in a reasonable time period. Therefore, for temperatures $\geq 150 \text{ °C}$, the entire $1.5 \mu\text{m}$ barrier was saturated with water to measure the saturated stress $\sigma(\infty)$. Saturation is reached when the stress no longer changes with exposure time. But at lower temperatures, saturating a $1.5 \mu\text{m}$ thick barrier with water can take

months. To overcome this disadvantage, a 100 nm thin barrier film on silicon wafer was tested. At temperatures less than 150 °C, this thinner barrier film was saturated within days for the measurement of the saturated stress $\sigma(\infty)$.

VIII. RESULTS

A. SIMS measurement

The hydrogen and deuterium SIMS profiles in a 660 nm thick barrier film, given in Fig. 4, were obtained after treatment in 101 °C boiling deuterium oxide for 12 h. The deuterium profile was fitted with a complementary error function. Deuterium (D) diffuses in with a diffusion coefficient D of $4.2 \times 10^{-15} \text{ cm}^2/\text{s}$ and a surface concentration of $7 \times 10^{20} \text{ atoms/cm}^3$. An as-deposited sample has a hydrogen concentration of $6.5 \times 10^{20} \text{ atoms/cm}^3$. Hydrogen (H) diffuses out of the barrier with the same diffusion coefficient of $4.2 \times 10^{-15} \text{ cm}^2/\text{s}$. The surface concentration of hydrogen is $2.5 \times 10^{20} \text{ atoms/cm}^3$. The profile of the sum of hydrogen and deuterium concentrations has the same diffusion coefficient of $4.2 \times 10^{-15} \text{ cm}^2/\text{s}$. By subtracting the background (as-deposited) hydrogen concentration of the barrier from the hydrogen+deuterium profile, the profile of excess hydrogen+deuterium that has diffused in was obtained. This excess hydrogen+deuterium has a surface concentration of $3.2 \times 10^{20} \text{ atoms/cm}^3$, which corresponds to a molecular concentration water in the surface of $1.6 \times 10^{20} \text{ molecules/cm}^3$ or 5 mg/cm^3 .

The H and ^{18}O SIMS profiles in a 660 nm thick barrier film were measured after a 4 h soak in boiling H_2^{18}O . Figure 5 shows the excess (above as-deposited) concentration profiles of H and ^{18}O and their *erfc* and exponential fits, respectively. The as-deposited concentration of hydrogen is $8.8 \times 10^{20} \text{ atoms/cm}^3$. The hydrogen follows a complementary error function with an excess surface concentration of $2 \times 10^{20} \text{ atoms/cm}^3$ and a diffusion coefficient of $3.5 \times 10^{-15} \text{ cm}^2/\text{s}$. The hydrogen diffusion profile is comparable to the SIMS profile obtained in the deuterium oxide diffusion experiment. The ^{18}O has a surface concentration of $1.8 \times 10^{21} \text{ atoms/cm}^3$. A good exponential fit can be made to the ^{18}O data beyond a depth of 50 nm into the barrier. There ^{18}O fits $e^{(-x/L)}$ with $L = 84 \text{ nm}$. Table III summarizes the results obtained from the H_2^{18}O diffusion experiment.

B. Electrical capacitance

Figure 6 shows the plot of $(1/C(t) - 1/C(0))^2$ as a function of time, for successive water exposure of one sample at 100 °C and 100% relative humidity. Table IV summarizes the results. The initial capacitance is 130 pF and the

TABLE II. Summary of results inferred from SIMS profiling after 12 h in boiling D_2O .

Atoms/molecules	Diffusion coefficient cm^2/s	Surface concentration atoms/cm^3	Background atoms/cm^3	Profile
Hydrogen	4.2×10^{-15}	2.5×10^{20}	6.5×10^{20}	<i>erfc</i>
Deuterium	4.2×10^{-15}	7.2×10^{20}	$<1 \times 10^{18}$	<i>erfc</i>
Hydrogen + deuterium	4.2×10^{-15}	9.7×10^{20}	6.5×10^{20}	<i>erfc</i>
Excess water (includes all isotopes)	4.2×10^{-15}	$1.6 \times 10^{20} \text{ molecules/cm}^3$ or $5 \times 10^{-3} \text{ g/cm}^3$	0	<i>erfc</i>

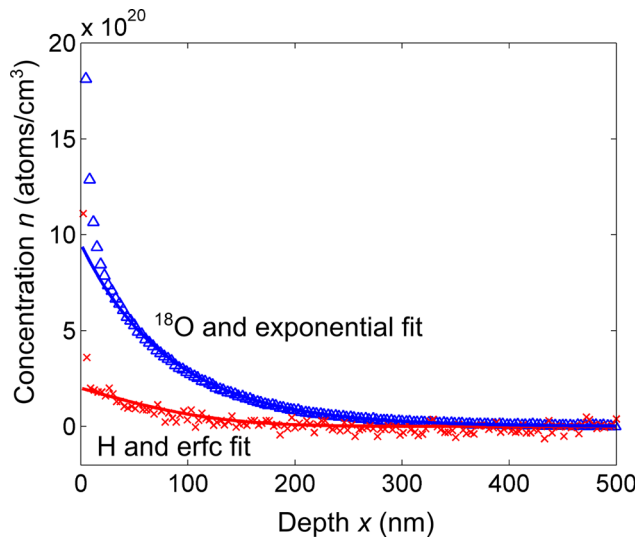


Fig. 5. (Color online) Excess (above as-deposited values) hydrogen and ^{18}O concentration profiles in a 660 nm thick barrier film on silicon a wafer after exposure to boiling H_2^{18}O for 4 h. The hydrogen fits an *erfc* function with a surface concentration of 2×10^{20} atoms/cm 3 , and a diffusion coefficient of 3.5×10^{-15} cm 2 /s. The excess ^{18}O fits the exponential $e^{(-x/L)}$ with a surface concentration of 9.5×10^{20} atoms/cm 3 and a characteristic length L of 84 nm.

saturated capacitance is 158 pF. The thickness of the dielectric $h = 200$ nm remained $\gg \sqrt{Dt}$ and was assumed to be constant. $C(\infty)$ was obtained by saturating capacitors in the water bath for 23 h at 100 °C. From the slope in Fig. 6, the diffusion coefficient is measured to be 5.6×10^{-15} cm 2 /s. The diffusion coefficient matches the value obtained from SIMS measurements within experimental error. The dielectric constant is calculated from the measured capacitance and capacitor dimensions. The apparently low initial dielectric constant of 3.7 in Table IV results from uncertainty in top chromium electrode area caused by shadow mask sputtering. The concentration calibration factor K_ϵ that relates the dielectric constant to solubility is $K_\epsilon = 5 \times 10^{-21}$ (molecules/cm 3) $^{-1}$.

C. Mechanical stress

Figure 7 shows the square of the change in film stress, $(\sigma(t) - \sigma(0))^2$, as a function of time for a 1.5 μm barrier held in a 100 °C boiling water bath. A 100 nm thick barrier saturated with boiling water for 40 h has 325 MPa compressive stress. The change in film stress follows a straight line, again confirming that the diffusion coefficient is independent of H_2O concentration. The diffusion coefficient extracted is

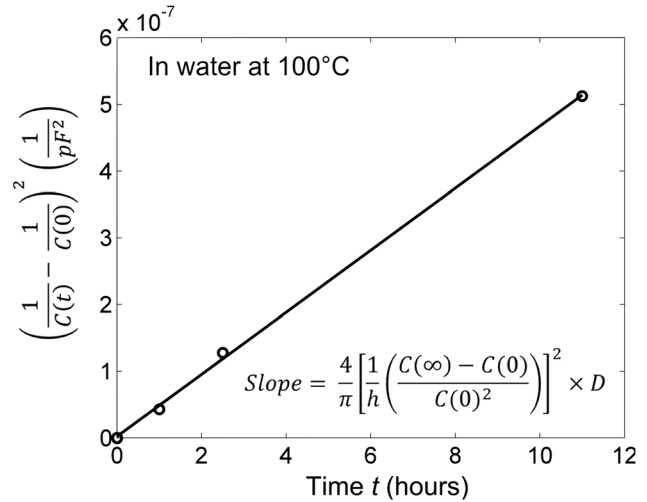


Fig. 6. Square of the inverse change in capacitance over time. The diffusion coefficient is 5.6×10^{-15} cm 2 /s.

4.4×10^{-15} cm 2 /s. This result matches well with the SIMS and capacitance results of 4.2×10^{-15} cm 2 /s and 5.6×10^{-15} cm 2 /s, respectively. Calibration of the saturated stress against the dissolved water concentration obtained from SIMS leads to $K_\sigma = 2 \times 10^{-18}$ MPa/(molecules/cm 3).

D. Thermal activation energies of solubility and diffusion coefficient

Samples with a 100 nm thick barrier were saturated with water at temperatures from 65 to 200 °C. Using the calibration factor K_σ , $(\sigma(0) - \sigma(\infty))$ was converted to surface concentration n_0 (or solubility S). Figure 8 shows its temperature dependence. As described in Sec. IV B, the concentrations obtained at 65 and 85 °C are normalized to 1 atmosphere by dividing by the saturated water vapor pressure at 65 and 85 °C, respectively. Stress measurements conducted below 100 °C show that at a fixed temperature the saturated stress is proportional to the vapor pressure. We assume that the saturated stress is proportional to the solubility with a proportionality constant that does not depend on the temperature. Then, the solubility has a thermal activation energy of -0.20 eV derived from Fig. 8. For a given water vapor pressure, the solubility falls with rising temperature.

The diffusion coefficients between temperatures 65 and 200 °C were measured using the mechanical stress measurement technique. Figure 9 is the plot of the diffusion coefficients versus inverse temperature. They follow an Arrhenius distribution. The thermal activation energy for the diffusion

TABLE III. Summary of results inferred from SIMS profiling after 4 h in boiling H_2^{18}O .

Atoms/molecules	Diffusion coefficient cm 2 /s	Surface concentration atoms/cm 3	Background atoms/cm 3	Profile
Oxygen-18 (^{18}O)	—	1.8×10^{21}	9×10^{19}	Oxygen exponential profile with a characteristic length of 84 nm
Hydrogen	3.5×10^{-15}	11×10^{21}	8.8×10^{20}	
Excess ^{18}O	—	9.5×10^{20}	0	
Excess hydrogen	3.5×10^{-15}	2×10^{20} molecules/cm 3	0	<i>erfc</i>

TABLE IV. Electrical capacitance of sample exposed to boiling water (100 °C and 100% relative humidity). The thickness of the barrier film in the capacitor is 200 nm.

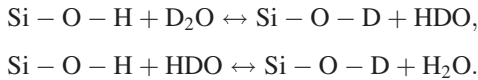
Parameter	Value	Parameter	Value
$C(0)$	130 pF	ϵ_0	3.7
$C(\infty)$	158 pF	$\epsilon(x, \infty)$	4.5
Dielectric thickness	200 nm	K_ϵ	$5 \times 10^{-21} \left(\frac{\text{molecules}}{\text{cm}^3}\right)^{-1}$
Area	$0.79 \times 10^{-2} \text{ cm}^2$		

coefficient is 0.71 eV. Note that the diffusion coefficients matches the value measured in fused silica by Davis and Tomozawa by infrared absorption measurements,³⁰ suggesting that the barrier material made at room temperature is similar to fused silica.

Table V summarizes the parameters of all stress experiments.

IX. DISCUSSION OF RESULTS

Figure 4 shows the out-diffusion of hydrogen with a concentration profile that follows a complementary error function. This is the consequence of hydrogen bonded in SiOH groups exchanging with deuterium from in-diffusing D₂O or HDO



Because this equilibration is fast even at low temperature, it does not change the diffusion coefficient of H₂O, HDO, or D₂O. The exchange generates H₂O, which diffuses farther into, or out of, the barrier with the same diffusion coefficient as in-diffusing D₂O.

In Fig. 4, the surface concentration of H is 2.5×10^{20} atoms/cm³. If the exchange reactions listed above had gone to completion the surface concentration of H (in equilibrium

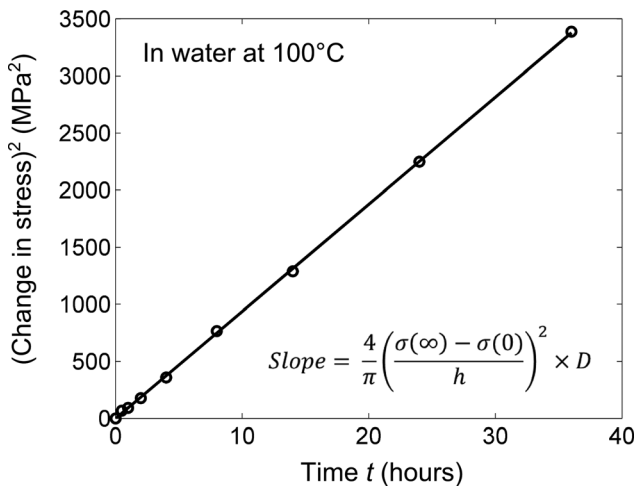


FIG. 7. Square of the change in stress vs time in hours [see Eq. (23)]. The 1.5 μm thick barrier film on silicon wafer was held in boiling water at 100 °C. The saturated stress was measured on a 100 nm thick barrier. The change in stress from as-deposited to saturation is -325 MPa. The diffusion coefficient is $4.4 \times 10^{-15} \text{ cm}^2/\text{s}$.

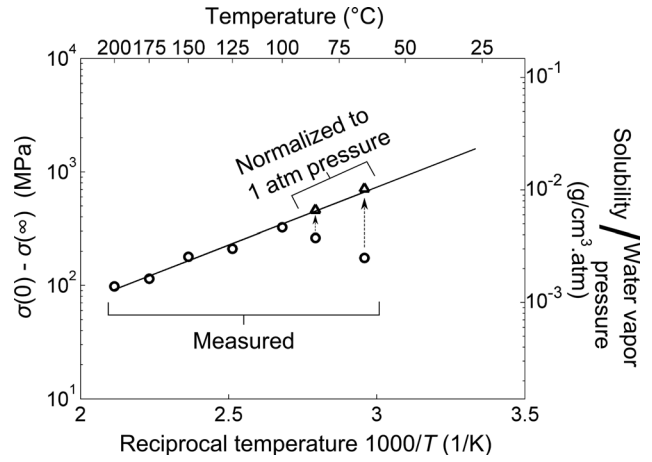


FIG. 8. Arrhenius plot of saturated stress (left scale) and normalized solubility (right scale): The circles denote the saturated stress at 1 atmosphere water vapor pressure above 100 °C, and at saturated vapor pressure below 100 °C. The triangles denote the saturated stress normalized to 1 atmosphere water vapor pressure. The line fit to the solubility of water has a thermal activation energy of -0.20 eV.

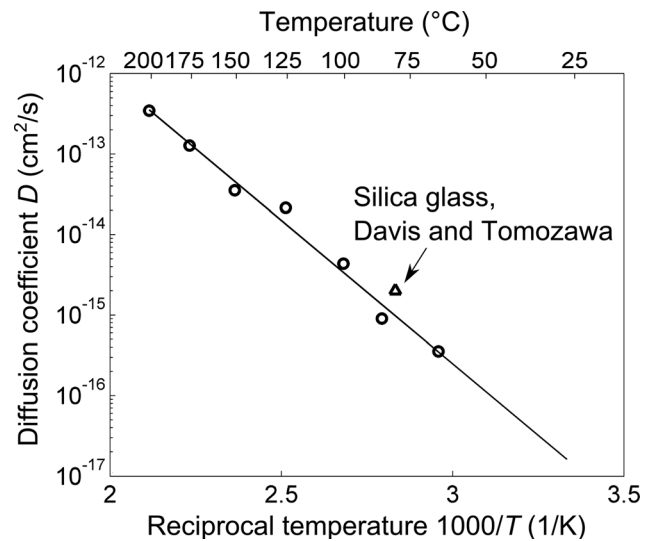


FIG. 9. Arrhenius plot of the diffusion coefficient determined by film stress measurements. The thermal activation energy determined from the slope is 0.71 eV. The triangle represents a value obtained by Davis and Tomozawa (Ref. 30) for fused silica.

TABLE V. Mechanical stress measurements on a sample exposed to boiling water at 100 °C and 100% relative humidity.

Parameter	Value
$\sigma(0)$	-90 MPa
$\sigma(\infty)$	-415 MPa
Silicon substrate	(100) 100 mm silicon 525 μm thick
K_σ	$2 \times 10^{-18} \frac{\text{MPa}}{\text{molecules/cm}^3}$
h	1500 nm
E_{S_0}	-0.20 eV
E_D	0.71 eV

with liquid D₂O) would have gone to zero. The observation that it has not suggests that some H in the barrier material may be immobile. Subtracting the H surface concentration of 2.5×10^{20} atoms/cm³ from the (D + H) sum at the surface, 9×10^{20} atoms/cm³, results in approximately the bulk concentration of H, which in Fig. 4 is 6.5×10^{20} atoms/cm³. This observation suggests that the mobile hydrogen in this sample has the concentration of 6.5×10^{20} atoms/cm³, while that of the immobile hydrogen is 2.5×10^{20} atoms/cm³.

The *erfc* concentration profiles of Fig. 4 reflect diffusion without reaction. However, the excess ¹⁸O concentration profile of Fig. 5 does not fit an *erfc*. It might fit an exponential function, as shown in Fig. 5. We interpret this exponential dependence to be the consequence of a reaction-diffusion process; ¹⁸O exchanges with the O of the Si-O-Si network; the network remains intact. The process is so slow that it will have no effect on the one-monolayer permeation time τ_{ML} .

The diffusion coefficient extracted from all three concentration profiles of Fig. 4 is identical. This suggests that H and D diffuse in the form of water molecules. The diffusion coefficients of H₂O, HDO, and D₂O are likely to be reciprocal to the square root of molecular weight, and therefore to exhibit negligible differences.

The diffusion coefficient is independent of the thickness of the film and of the measurement technique. The capacitance measurement done on a 200 nm thick film and the stress measurement done on a 1 μ m film result in the same diffusion coefficient. The diffusion coefficient is also independent of the concentration of dissolved water between temperatures 65 and 200 °C. The complementary error function observed in SIMS and the quadratic change of inverse capacitance and of stress with exposure time imply that the diffusion coefficient is independent of concentration. There is no evidence of reaction-diffusion mechanism, except for the ¹⁸O profile of Fig. 5.

In summary, evidence points to processes 1–4 of Sec. III to happen, and process 5 only beginning to happen, in our barrier films up to the temperature of 200 °C.

The question remains if water might have penetrated via defects in the film or along the film/substrate interface.¹⁵ If defects had affected our results, the experiment with quite different samples, conducted over areas that ranged from $125 \times 125 \mu\text{m}^2$ (SIMS) to 0.01 cm^2 (capacitance) to 4 in. diameter wafer (stress) would have yielded different values of *D*.

In the three groups of experiments, along interfaces, water would have to diffuse sideways from the edges of the sample over distances in the order of centimeters. Because this length is much larger than the top–down diffusion distance through the bulk of the barrier, the likelihood of “sideways” interface diffusion affecting our results is small. The absence of deuterium at the bottom interface with the substrate in the SIMS experiments shown in Fig. 4 confirms the absence of such interface diffusion. Modeling interface diffusion¹⁵ reaches the same conclusion when a typical diffusion coefficient of $10^{-8} - 10^{-7} \text{ cm}^2/\text{s}$ is used.

X. MODELING THE ONE MONOLAYER PERMEATION TIME

The permeation barrier is designed to protect OLEDs for longer than 10 years under actual conditions of use. Such lifetimes clearly are too long for experimentation. Knowing the solubility and its activation energy, the diffusion coefficient and its activation energy enables extrapolating the barrier performance from our experimental conditions to room temperature. The properties of the barrier at a demanding operating condition and two accelerated test conditions are listed in Table VI. For a 3 μ m thick barrier, the water vapor transmission rate and the lag-time are shown. The units for *WVTR* have been converted from molecules/cm²s to g/m²day.

From the solubility and diffusion coefficients and at a given temperature and relative humidity, the quantity of water that has diffused into a barrier by any given time can be calculated using Eq. (5). The time, τ_{ML} , taken by one-monolayer of water to permeate a 3 μ m barrier at 100% relative humidity, as a function of temperature, is given in Fig. 10.

τ_{ML} decreases upon increase in temperature and relative humidity. The factor of decrease in lifetime from a room temperature = T_{room} , and relative humidity = RH_{room} , to higher accelerated test temperature = $T_{\text{accelerated}}$, and relative humidity = $RH_{\text{accelerated}}$, is the acceleration factor

$$\text{Acceleration factor} = \frac{\tau_{ML}(T_{\text{room}}, RH_{\text{room}})}{\tau_{ML}(T_{\text{accelerated}}, RH_{\text{accelerated}})}. \quad (24)$$

The acceleration factor for different accelerated test temperatures, $T_{\text{accelerated}}$, when $RH_{\text{accelerated}} = 100\%$, $T_{\text{room}} = 38^\circ\text{C}$, and $RH_{\text{room}} = 90\%$ is calculated and is shown in Fig. 11.

TABLE VI. Barrier properties at three different temperature and relative humidity (*RH*) combinations. *WVTR*, lag-time and one monolayer permeation time are calculated for a 3 μ m thick barrier film.

	Diffusion coefficient cm ² /s	Surface concentration mg/cm ³	<i>WVTR</i> g/m ² /day	Lag-time	One-monolayer permeation time
Extreme operating condition:					
38 °C 90% RH	5.4×10^{-17}	0.97	1.5×10^{-7}	8.8 years	13.4 years
Accelerated test conditions:					
60 °C 90% RH	3.1×10^{-16}	3.6	3.2×10^{-6}	1.5 years	1.4 years
85 °C 85% RH	1.7×10^{-15}	3	1.5×10^{-5}	102 days	92 days

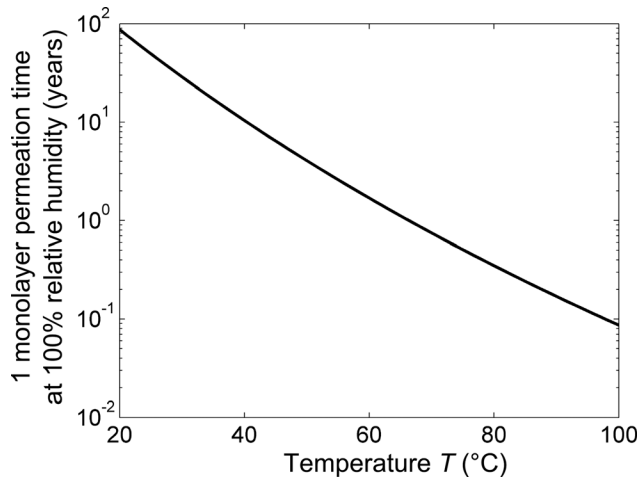


Fig. 10. Time taken for one monolayer of water to permeate a $3\ \mu\text{m}$ barrier at different temperatures and 100% relative humidity.

Another question of practical relevance is the time taken by one monolayer of water to permeate through barriers of different thicknesses at $38\ ^\circ\text{C}$, 90% relative humidity; this is given in Fig. 12 as time in function of barrier thickness. The time taken does not go linearly with thickness as one might expect from Eq. (7) for *WVTR*, or with the square of thickness as the diffusion length $L = \sqrt{Dt}$ would suggest. Instead the exponent of thickness (1.57 in the case of Fig. 11) lies between 1 and 2. This is because most of the duration of exposure to water, up to the lag-time, the water permeation is not in steady state (see Fig. 2). The lag-time varies quadratically with the thickness as given by Eq. (8). As a result in our specific case, τ_{ML} varies with thickness with an empirically fitted exponent of 1.57, at $38\ ^\circ\text{C}$, and 90% relative humidity

$$\tau_{ML} = 2.14 \times h^{1.57}. \quad (25)$$

This example shows that the steady state water vapor transmission rate is an inadequate gauge for quantifying

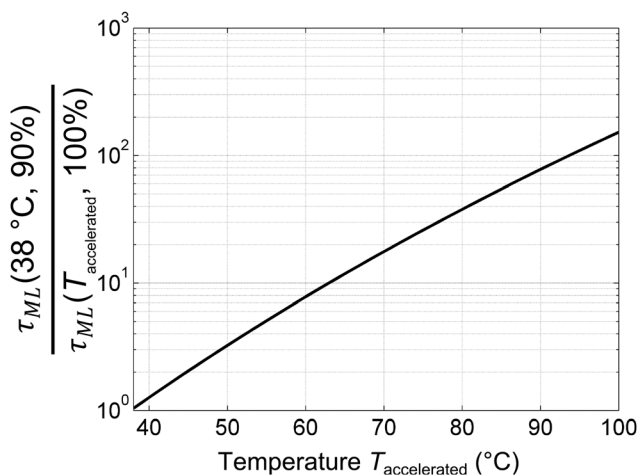


Fig. 11. Ratio of one-monolayer lifetime at $38\ ^\circ\text{C}$, 90% relative humidity and high temperature test conditions, 100% relative humidity is plotted versus temperature for a $3\ \mu\text{m}$ barrier.

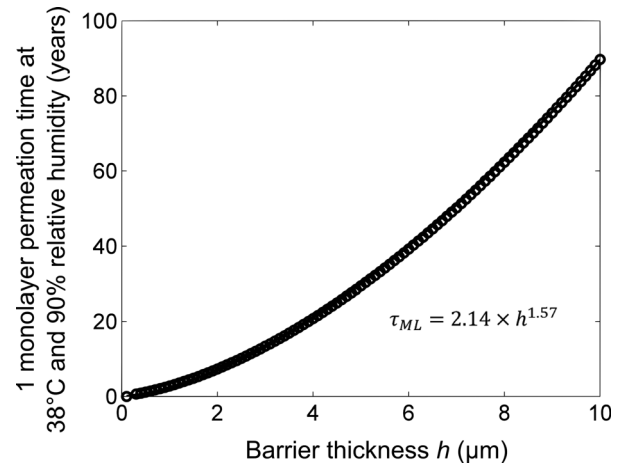


Fig. 12. Thickness dependence τ_{ML} . The time scales exponentially with thickness with an exponent of 1.57.

ultralow barriers. τ_{ML} provides a more realistic gauge as combines the effect of lag time and *WVTR*. Once the solubility and the diffusion coefficient for a barrier material at operating conditions are known, a barrier can be designed that meets the required permeation target. Our target is a maximum one monolayer of water permeation over a 10 year device lifetime at $38\ ^\circ\text{C}$, 90% relative humidity. A $3\ \mu\text{m}$ thick barrier of the material we studied here would have a one-monolayer permeation lifetime, τ_{ML} , of 13.4 years.

XI. CONCLUSIONS

We have developed quantitative tools for measuring and modeling the diffusion of water through a permeation barrier. We demonstrated these tools on barrier layers made from one particular SiO_2 -silicone hybrid material. The measurement tools include SIMS, which is needed for calibration of the hydrogen concentration in the layers, and also is used for a determination of the diffusion coefficient. Measurements of electrical capacitance and mechanical film stress provide the concentration of water, after a one-time calibration with SIMS, and changes in capacitance and stress enable the determination of the diffusion coefficient. Exposing films to water at high temperature and high humidity accelerates the laboratory measurements. Their results are employed in a model that predicts water permeation under the typical operating conditions of flexible OLED displays and of other devices that require flexible barriers with extremely low permeability.

ACKNOWLEDGMENT

Bhadri Visweswaran gratefully acknowledges the fellowship support from the Princeton Program in Plasma Science and Technology.

¹D. Kolosov, D. S. English, V. Bulovic, P. F. Barbara, S. R. Forrest, and M. E. Thompson, *J. Appl. Phys.* **90**, 3242 (2001).

²P. E. Burrows, V. Bulovic, S. R. Forrest, L. S. Sapochak, D. M. McCarty, and M. E. Thompson, *Appl. Phys. Lett.* **65**, 2922 (1994).

³M. S. Weaver *et al.*, *Appl. Phys. Lett.* **81**, 2929 (2002).

- ⁴Y. Leterrier, Y. Wyser, J. A. E. Manson, and J. Hilborn, *J. Adhes.* **44**, 213 (1994).
- ⁵Y. Leterrier, *Prog. Mater. Sci.* **48**, 1 (2003).
- ⁶A. G. Erlat, R. J. Spontak, R. P. Clarke, T. C. Robinson, P. D. Haaland, Y. Tropsha, N. G. Harvey, and E. A. Vogler, *J. Phys. Chem. B* **103**, 6047 (1999).
- ⁷Y. Leterrier, L. Boogh, J. Andersons, and J. A. E. Manson, *J. Polym. Sci., Part B: Polym. Phys.* **35**, 1449 (1997).
- ⁸Y. Leterrier, J. Andersons, Y. Pitton, and J. A. E. Manson, *J. Polym. Sci., Part B: Polym. Phys.* **35**, 1463 (1997).
- ⁹J. Affinito, "Environmental barrier material for organic light emitting device and method of making," U.S. patent 6,268,695 (31 July 2001).
- ¹⁰T. Harvey, S. Shi, and F. So, "Hermetic sealing of plastic substrate," U.S. patent 5,686,360 (11 November 1997).
- ¹¹A. B. Chwang *et al.*, *Appl. Phys. Lett.* **83**, 413 (2003).
- ¹²G. L. Graff, R. E. Williford, and P. E. Burrows, *J. Appl. Phys.* **96**, 1840 (2004).
- ¹³P. Mandlik, J. Gartside, L. Han, I. C. Cheng, S. Wagner, J. A. Silvernail, R. Q. Ma, M. Hack, and J. J. Brown, *Appl. Phys. Lett.* **92**, 103309 (2008).
- ¹⁴L. Han, P. Mandlik, J. Gartside, S. Wagner, J. A. Silvernail, R. Q. Ma, M. Hack, and J. J. Brown, *J. Electrochem. Soc.* **156**, H106 (2009).
- ¹⁵P. Mandlik, L. Han, S. Wagner, J. A. Silvernail, R. Q. Ma, M. Hack, and J. J. Brown, *Appl. Phys. Lett.* **93**, 203306 (2008).
- ¹⁶R. S. Kumar, M. Auch, E. Ou, G. Ewald, and C. Soo Jin, *Thin Solid Films* **417**, 120 (2002).
- ¹⁷J. H. Choi, Y. M. Kim, Y. W. Park, J. W. Huh, B. K. Ju, I. S. Kim, and H. N. Hwang, *Rev. Sci. Instrum.* **78**, 064701 (2007).
- ¹⁸R. Paetzold, A. Winnacker, D. Henseler, V. Cesari, and K. Heuser, *Rev. Sci. Instrum.* **74**, 5147 (2003).
- ¹⁹R. L. Hamilton, *Bell Syst. Tech. J.* **46**, 391 (1967).
- ²⁰R. Dunkel, R. Bujas, A. Klein, and V. Horndt, *Proc. IEEE* **93**, 1478 (2005).
- ²¹M. D. Groner, S. M. George, R. S. McLean, and P. F. Carcia, *Appl. Phys. Lett.* **88**, 051907 (2006).
- ²²P. E. Burrows *et al.*, *Displays* **22**, 65 (2001).
- ²³R. H. Doremus, *J. Mater. Res.* **14**, 3754 (1999).
- ²⁴J. Crank, *The Mathematics of Diffusion*, 2nd ed. (Clarendon, Oxford, 1975), p. viii.
- ²⁵R. H. Doremus, *J. Mater. Res.* **10**, 2379 (1995).
- ²⁶J. Fraden, *Handbook of Modern Sensors: Physics, Designs, and Applications*, 3rd ed. (Springer, New York, 2004).
- ²⁷L. D. Landau and E. M. Lifshits, *Electrodynamics of Continuous Media* (Pergamon, New York, 1960), Vol. 8, p. 45.
- ²⁸L. Hartshorn, N. J. L. Megson, and E. Rushton, *J. Soc. Chem. Ind.* **56**, 266T (1937).
- ²⁹G. G. Stoney, *Proc. R. Soc. London, Ser. A* **82**, 172 (1909).
- ³⁰K. M. Davis and M. Tomozawa, *J. Non-Cryst. Solids* **185**, 203 (1995).